AD-A097 713 EMMANUEL COLL BOSTON MA F/G 4/1
AURORAL X-RAY CONTAMINATION OF THE LOW ENERGY PROTON SPECTROMET--ETC(U)
JAN 81 R P BOYLE, D R PARSIGNAULT F19628-79-C-0102
UNCLASSIFIED SCIENTIFIC-2 AFGL-TR-80-0265 NL

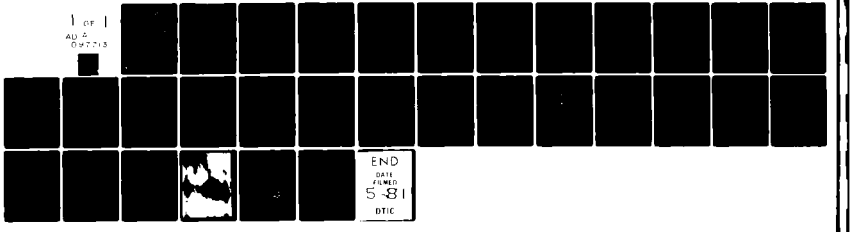

AFGL-TR-80-0265

LEVEL II

(12)

Auroral X-Ray Contamination of the Low Energy Proton Spectrometer on the S3-2 Satellite in the Polar Regions

Richard P. Boyle

Daniel R. Parsignault

The Trustees of Emmanuel College
400 The Fenway
Boston MA 02115

January 1981

Scientific Report No. 2

Approved for public release; distribution unlimited.

Air Force Geophysics Laboratory
Air Force Systems Command
United States Air Force
Hanscom AFB Massachusetts 01731

(14) SCIENTIFIC-2

MIL-STD-847A
31 January 1973

UNCLASSIFIED
SECURITY CLASSIFICATION OF THIS PAGE (When Data Entered)

(19) REPORT DOCUMENTATION PAGE

READ INSTRUCTIONS BEFORE COMPLETING FORM

1. REPORT NUMBER (18) AFGL-TR-80-0265	2. GOVT ACCESSION NO. AD-A097 423
	3. RECIPIENT'S CATALOG NUMBER
4. TITLE (and Subtitle) (6) Auroral X-Ray Contamination of the Low Energy Proton Spectrometer on the S3-2 Satellite in the Polar Regions	5. TYPE OF REPORT & PERIOD COVERED Scientific Report No.2 01JAN80 - 31AUG80
	6. PERFORMING ORG. REPORT NUMBER
7. AUTHOR(s) (10) Richard P. Boyle, Daniel R. Parsignault (15)	8. CONTRACT OR GRANT NUMBER(s) F19628-79-C-0102
9. PERFORMING ORGANIZATION NAME AND ADDRESS Emmanuel College, 400 The Fenway, Boston MA 02115 (12) 11	10. PROGRAM ELEMENT, PROJECT, TASK AREA & WORK UNIT NUMBERS 61102F (16), 2311G1AK (17) 62
11. CONTROLLING OFFICE NAME AND ADDRESS Air Force Geophysics Laboratory, Hanscom AFB MA 01731, PHG, Contract Monitor: Robert O. Hutchinson (11)	12. REPORT DATE 31 Jan 1981
	13. NUMBER OF PAGES 30
14. MONITORING AGENCY NAME & ADDRESS (if different from Controlling Office) (9) Rept. for 1 Jan-31 Aug 80	15. SECURITY CLASS (of this report) Unclassified
	15a. DECLASSIFICATION/DOWNGRADING SCHEDULE

16. DISTRIBUTION STATEMENT (of this Report)

A - Approved for public release; distribution unlimited.

17. DISTRIBUTION STATEMENT (of the abstract entered in Block 20, if different from Report)

TECH, OTHER

18. SUPPLEMENTARY NOTES

19. KEY WORDS (Continue on reverse side if necessary and identify by block number)

Auroral X-Rays
Bremsstrahlung
S3-2 Satellite
LEPS (Low Energy Proton Spectrometer)
Electron Precipitation

20. ABSTRACT (Continue on reverse side if necessary and identify by block number)

The Low Energy Proton Spectrometer (LEPS) on board the Air Force S3-2 polar orbiting satellite recorded, at polar latitudes, ~~(invariant latitude > 70°)~~, high anomalous counts coming from the auroral zone direction, over the December 1975 through April 1976 operational period. Despite the low sensitivity of the Si(Li) LEPS detector to X-rays, bremsstrahlung from

DD FORM 1473 EDITION OF 1 NOV 65 IS OBSOLETE

UNCLASSIFIED
SECURITY CLASSIFICATION OF THIS PAGE (When Data Entered)

12893

precipitating electrons in the hundred keV energy range is given as the source of these observations.

TABLE OF CONTENTS

	Page
ABSTRACT	3
1. INTRODUCTION	4
2. OBSERVATIONS	5
3. DETECTOR SENSITIVITY	7
4. ANALYSIS	8
5. CONCLUSION	12
6. ACKNOWLEDGEMENTS	13
REFERENCES	14
LIST OF FIGURES	15
FIGURES AND TABLE	17

1. INTRODUCTION

A low energy proton spectrometer (LEPS) was flown on the Air Force S3-2 polar orbiting satellite to observe primarily the trapped protons in the 0.1 to 6 MeV energy range (Pantazis et al., 1975). In the polar regions, which usually showed low proton fluxes, the LEPS recorded high counts in a single direction below the satellite horizon over the course of the five-month operational period. The same pattern of observations can be seen in the work of Imhof et al. (1974), where a Ge(Li) spectrometer was used to observe bremsstrahlung X-rays from the auroral zones. Although the LEPS is theoretically inefficient in detecting X-rays, in this report we contend that it is the X-ray aurora that best explains qualitatively the dominant feature of the LEPS polar observations.

During the last decade several researchers have correlated observed electron spectra with observed X-ray spectra in the auroral zones. In such research, bremsstrahlung X-ray measurements provide a broader picture of the auroral zones than the more spatially limited electron observations. This report offers qualitative observational information on the subject of the correlation between precipitating electrons and the emerging bremsstrahlung X-rays as observed by detectors on the S3-2 satellite.

The Air Force S3-2 satellite was launched December 5, 1975 into a polar orbit in the noon-midnight meridian with an apogee of 1540 km, perigee of 230 km, inclination of 96.3 degrees, and a period of 1.71 hours. The ascending node was on the nighttime equator. The satellite spin period was approximately 18.5 seconds, with the spin axis perpendicular to the orbital plane.

The LEPS provided useful proton observations in the trapping and precipitating latitudes during the operational period from launch, December 1975 to May 1976. However, in the polar regions, here defined as poleward of the precipitating regions, although evidence of any solar proton fluxes is sparse and restricted to solar active periods, the observation of varying high counts from a single preferred direction below the satellite horizon persists throughout the five month period. This report explains that these anomalous polar observations

are the result of electromagnetic radiation, namely, bremsstrahlung X-rays originating in the auroral zones.

The following section gives a description of the LEPS polar observations. Since the most statistically significant counts are contained in the first energy channel (100 $\pm$ 20 keV), we will concentrate on that energy channel. Usually, only the first six channels have statistically significant counts (82 keV $<$ E $<$ 680 keV). Evidence that the observations must be due to the electromagnetic radiation necessitates the evaluation of the finite sensitivity of the LEPS to X-rays in the hundred keV energy range. Analysis of the observations will then give confirmation that X-ray aurorae and not solar particles, per se, are what were observed. Because of the low efficiency of this detector to X-rays, however, only qualitative, order of magnitude conclusions on these polar observations of the X-ray aurorae can be made.

2. OBSERVATIONS

From roughly 1100 S3-2 data tapes processed by the Air Force Geophysics Lab., 245 tapes, each containing a partial or full orbit during the 10 December 1975 to 26 April 1976 operational period for the LEPS, have been further processed. Figure 1 shows a typical data record of the spin-modulated counting rates plotted as a function of time for a northern hemisphere pass in the 100 keV energy channel of the LEPS. Night and day trapping, precipitating and polar regions are indicated in the figure. This pass shows a symmetry in the polar observations between night and day. In the northern hemisphere, orbital passes during the time interval of 18 to 24 hours UT fell close to the midnight-noon magnetic meridian. Orbital passes outside of this universal time interval fell toward the evening sector away from the midnight-noon magnetic meridian. Symmetry of the polar observations in passing from the night to dayside of the magnetic pole correlates well with the closeness of the orbit to the midnight-noon magnetic meridian. In contrast to the data shown in Figure 1, the dynamic range of the polar counts is demonstrated by the April 17, 1976 polar pass (cf Fig. 2) which shows minimal (near zero) counts during the time of very low

magnetic activity (Kp = 2-). In general, a correlation existed between the magnitude of the polar counts and the magnitude of the planetary magnetic three-hour-range indices, Kp, reproduced in Figure 3 for the five month period under consideration. In their recent work, Imhof et al. (1980) present evidence that the local dusk sector experiences the more intense electron precipitation, and hence X-ray bremsstrahlung, compared to any other local geomagnetic time region. The S3-2 LEPS north polar observations during the five months observing period tend to add evidence to this case. The S3-2 orbit did not traverse the northern dawn sector. But the comparison of the polar observations from orbits over late night to late morning vs. early evening to noon show that the dusk sector gives the relatively higher counts (proportional to the Kp of the time).

In Figure 4, a plot of the range in invariant latitude, local geomagnetic time covered by the satellite's north polar orbits is demonstrated. The $9^h \pm 3^h$ UT pass represents one extreme where the orbit passes along the dusk side over the auroral oval. The $21^h \pm 3^h$ UT pass gives the other extreme where a late evening to late morning crossing over the auroral oval is made. Orbits at other universal times lie in between these extremes. Approximate invariant latitude and local geomagnetic time for any of the counts vs. time plots, given its universal time, can be read off the auroral oval nomograph of Figure 4.

Figure 5 gives a representative selection of the data from the north polar region for the five month period. For active to quiet magnetic Kp indices, column A demonstrates the data for the dusk side passes and column B for the late evening to late morning passes.

The counts/second over a single 18-second spin period in the polar region show an asymmetric distribution with a persistent single enhanced peak (cf. print plot, Figure 10). In contrast, a monoenergetic beam of charged-particle radiation in the presence of a magnetic field and hence spiraling particles, must show a double peak of equal intensity to a detector viewing around a plane (cf. Figure 6). The spiraling charged radiation would give equal intensity peaks at $\pm$ 90° pitch angle. Although the LEPS polar observations usually contain two peaks within

a single spin, they are neither of equal intensity nor separated by $\pm$ 90° pitch angle. The peaks occur at pitch angles of -120° and +110° in the north night and day, respectively, and at pitch angles of -80° and +70° in the south night and day, respectively. Although this is a difference of only 10°, nevertheless the argument for a single peak is corroborated from the strong connection of the look direction angle of the peak to the geometrical location of the auroral zone. This will be explained more fully in a later section. Thus, the evidence is that the peak observation is not of charged particles, i.e., protons or electrons, but rather, is from viewing two discrete sources of electromagnetic radiation at two different directions.

3. DETECTOR SENSITIVITY

The LEPS was designed to detect and analyze protons in the 0.1 to 6 MeV energy range. Two totally depleted Si(Li) surface barrier detectors were used in an anticoincidence mode. Full description of the instrument can be found in Pantazis et al. (1975). Table 1 gives the energies of the eleven channels of the LEPS. The wide angle (46°) LEPS instrument on the S3-2 satellite gave useful proton observations in the high flux, trapping and precipitating regions during the five month operational period. The anomalous single peak observations in the polar regions raise the question of the sensitivity of the LEPS to X-rays.

An incident X-ray can generate an electronic charge in the detector's sensitive volume in three energy-dependent ways: by the photoelectric effect, by the Compton effect, and by pair-production. The fact that pair-production occurs above 1.1 MeV, where the LEPS in the polar regions sees no counts, makes it unnecessary to consider it here. Figure 7 shows the percent efficiency to charge generation from the photoelectric and Compton effects in the 300 μ silicon front detector. These curves are computed from the transmission equation

$$N = N_0 e^{-\mu x}$$

where N_0 = number of incident photons at a particular energy,

N = number of transmitted photons,

μ = absorption coefficient in silicon for particular energy,

x = thickness of silicon.

It can be seen that the LEPS is about an order of magnitude more sensitive to electron charge generation by Compton scattered electrons than by photoelectrons at 100 keV. At higher energies the photoelectric effect is a much less efficient source of electron generation. Consequently, charge in the front detector, primarily due to Compton scattered electrons from an incident X-ray source, would give pulses or counts in the 100 keV to 6 MeV energy channels. Clearly, the LEPS is not immune to X-rays. In fact, in a space region devoid of protons, an X-ray flux could account for a significant counting rate by Compton scattering alone.

4. ANALYSIS

The source of the single peak polar observation will be explored and discussed in this section. For a detailed analysis we have selected the data acquired during a north polar pass in a magnetically active time. The same considerations and results to be expressed here apply, in form, to all the polar regions both north and south during the five month period.

The single peak observation by the LEPS when in the polar region is not due to a source local to the satellite. Protons cannot be a local source for two reasons. First, another experiment onboard the same S3-2 satellite showed that the proton flux, specifically at 100 keV, in the polar region was at background level with no preferential pitch angle peak (A.L. Vampola, private communication). Second, as stated earlier, a proton flux at any one energy and a preferred direction would show at least a double peak of equal intensity at pitch angles $\pm$ °. The fact that the LEPS efficiently and accurately observed the proton flux outside the polar region is reason enough that any proton flux within the polar region would also be seen.

Likewise, electrons can be ruled out as a local source of the LEPS single-peak polar observations - either directly or as a source of local bremsstrahlung. Directly, the LEPS is immune to seeing electrons by

being equipped with a 1400 gauss sweeping magnet. This magnetic shielding efficiently swept away electrons up to 600 keV in the high flux trapping region, i.e., the trapped proton observations by the LEPS were uncontaminated by electron counts. Local bremsstrahlung cannot be a source of the single peak for two reasons. First the energetic electron flux seen by another experiment onboard the same S3-2 satellite (A.L. Vampola, private communication), while in the polar region, was at a low level. Second, if the LEPS were sensitive to local bremsstrahlung generated by the low-level electron flux despite the reasonably adequate shielding of the LEPS, then presumably the observation would be more or less omni-directional and not at the single significant direction. Furthermore, the same sensitivity would be apparent in the trapped radiation regions where there are large fluxes of trapped electrons. The single preferred (consistently recurrent) direction of the polar observation is in fact explained in the following text by a source remote to the satellite, namely, the X-ray aurora.

It is known that the auroral zone emits X-rays isotropically by the bremsstrahlung process due to precipitating electrons incident on the atmosphere at approximately 100 km altitude. The single peak observed by the LEPS in the polar region is evidence of its sensitivity to electromagnetic radiation in the X-ray (100 keV) energies; the preferred direction of this single peak observed from various orbital vantage points is precisely the direction of the aurora.

Because of the extreme magnetic activity, we analyze in detail the data of orbit 1569 on March 26, 1976, 9^h UT in the following discussion (cf. Figure 8). Figure 9 shows to scale, in the orbiting plane, the north polar pass of the orbit 1569. The look angle from the local nadir at which the single peak is seen is portrayed from four orbital vantage points (a,b,c,d). Figure 10 shows the 100 keV observations during a single spin corresponding to the four vantage points. Here pitch angles are given.

As the satellite passes in the night side, from south of the aurora where the peak occurs at look angle +84° off the nadir to the north of the aurora where the peak is seen at -65° off the nadir, the angle of the peak might be expected to move through zero degrees. However, with the LEPS aperture of 46° at an altitude of approximately 1200 km, less

area of the aurora is in view when overhead than when oblique. Furthermore, when the aurora is viewed perpendicularly compared to nearly horizontally to its area, a decrease in X-ray intensity greater than an order of magnitude occurs. This effect is presented in detail by the recent work of Walt et al. (1979) who show that bremsstrahlung X-rays escape the auroral zone preferentially at angles near the horizontal. Also, this effect is more pronounced for the higher photon energies. At vantage point c (cf. Figure 9), the dayside peak has increased to a brightness equal to the decreasing nightside peak. As the satellite moves on to vantage point d, the look angle tends to move slightly closer to the nadir (from +65° now to +60°) before the single peak is covered by the precipitating and trapping proton fluxes.

The auroral zone is located within the field of view of the 46° aperture of the LEPS when pointing at these look angles both for the night and dayside aurorae. Corroboration of this fact is obtained from the location of the precipitating electron regions given by two electron experiments on board the same S3-2 satellite for the same March 26, 1976 orbital pass as well as from a DMSP photograph of the visible aurora. Electron observations in the 36 to 317 keV energy range (A.L. Vampola, private communication) locate the precipitating, and consequently auroral, region between 49 to 61° magnetic latitude. Observations from an electron sensor in the 80 eV to 17 keV energy range (R. Vancour, private communication) locate the precipitating region between 52° and 60° magnetic latitude. The DMSP photograph (cf. Figure 11) of the visible aurora from an orbital pass crossing the same nighttime auroral area as the S3-2 satellite and just 25 minutes after the S3-2 pass puts the equatorward edge of the bright continuous aurora at a corrected geomagnetic latitude of 58°. Bright discrete arcs and bands are observed poleward to 68°. The sudden commencement of the major geomagnetic storm began at 0233 UT. The Ap value reached 138, making it the fifth highest value of the 20th solar cycle. The planetary magnetic three-hour-range index, Kp, for this date remained high for 24 hours. The earth's polar cap underwent a very large expansion during this storm. In Figure 12, both the S3-2 and DMSP orbits are plotted on the auroral

oval nomograph (Whalen, 1970) for the largest polar cap expansion given for a complete oval (Q=7). The discrete arcs and bright continuous aurora have been sketched in from the photograph to show that for this storm the auroral oval has expanded even more than indicated in the nomograph.

We have attempted to compute a predicted bremsstrahlung X-ray flux at the LEPS aperture given the observed precipitating electron flux. The observed count rate for the point under study is 10^4 cts/sec. This occurs at altitude ~900 km, magnetic latitude ~70°, and UT ~ 9^h. An arrow on Figure 8 points out the time under study for the forthcoming comparison of observed vs. predicted count rate at the LEPS. A "best case" approach in estimating the configuration of the LEPS with respect to the auroral zone is taken in order to maximize the predicted count rate result. Referring to Figure 13, the opening angle of the LEPS is 46° and the subtended arc is

$$\ell = 2r \sin \frac{1}{2}\theta = 2(2886 \text{ km}) \sin 23°$$

$$\ell = 2255 \text{ km},$$

assuming the satellite is 26° poleward from the average latitude of the aurora. From the S3-2 electron data of Vampola (private communication) the extent of the precipitating zone is approximately 15° in latitude or 1665 km. Thus, the emitting volume is 2255 km × 1665 km = 3.75×10^{16} cm^2. Based on the electron observations for the date, the flux of precipitating electrons over this auroral zone is, on the average, 3.5×10^6 electrons/cm^2-sec. From the area in view of the LEPS, the total electron flux is $\Phi = 1.3 \times 10^{23}$ electrons/sec. The total area A, of a sphere centered on the auroral area and having a radius equal to the satellite distance away is 1.05×10^{18} cm^2. Thus, $\Phi/A = 1.25 \times 10^5$ electrons/cm^2-sec. We assume an isotropic distribution of the bremsstrahlung flux and further neglect the atmospheric absorption (justified because of the high (100 keV) energy considered along with the very small residual atmosphere between 100 km and the satellite altitude). In order to obtain the bremsstrahlung flux at the detector we use the numbers calculated by Berger and Seltzer (1972), $\Phi(K)/J_o \text{keV}^{-1}$, the differential bremsstrahlung flux per unit incident electron current and multiply by the above computed factor 1.25×10^5. The e-folding

energy obtained from the electron data is approximately 40 keV. Thus $\Phi(K)/J_o$ keV^{-1} differential is 7×10^{-7}. The total bremsstrahlung flux computed for the 100 keV (ΔE = 41 keV) channel of the LEPS is

$$7 \times 10^{-7} \frac{\text{photons}}{\text{electrons} \cdot \text{keV}} \times 1.25 \cdot 10^{5} \frac{\text{electrons}}{\text{cm}^2 \cdot \text{sec}} \cdot 41 \text{ keV} \cdot 2\text{cm}^2 \cdot \epsilon$$

$$7.2 \frac{\text{photons}}{\text{sec}} \cdot \epsilon, \text{ where } \epsilon = \text{efficiency of detector}$$

Referring to Figure 7 shows that the expected percent efficiency of the LEPS to 100 keV photoelectrons is only 0.2%. (A laboratory calibration of the LEPS for its sensitivity to X rays was not performed.) The final predicted photon counts/sec for this date of interest is

$$7.2 \times 0.2\% = 0.0144.$$

Thus there exists a great discrepancy between the predicted value of approximately 10^{-2} cts/sec and the observed value of approximately 10^{4} cts/sec.

5. CONCLUSION

This study has shown that the LEPS is considerably more sensitive to X-rays than initially predicted.

A possible reason for this discrepancy could be that the Berger and Seltzer calculation assumes a simple exponential spectrum for the precipitating electrons. Some actual measurements, however, show a two (or more) component electron spectrum which probably results in a higher X-ray production rate. Also, this instrument was not carefully calibrated for X-rays prior to launch. There may be inherent design characteristics that result in a higher than expected counting rate by X-radiation. Compton scattering in the detector might well be a source of some of the counts adding up in the various energy channels, but this in itself does not resolve the discrepancy. The fact that the LEPS recorded a signal at times as large as 2×10^{4} cts/sec in the auroral direction warrants attention in designing and operating any detectors similar in design and construction to the LEPS and operating them in any orbital configuration similar to that of the S3-2 satellite.

Finally, the relatively certain results in this study of the five

months observations are: the single high peak is always seen in the auroral zone direction; the peak is more intense the greater the Kp index, and the dynamic range of auroral X-rays of four or five orders of magnitude found in other auroral X-ray studies seems to be found in these observations.

6. ACKNOWLEDGEMENTS

Special thanks are given to D.F. Smart and M.A. Shea of AFGL for their direction and advice during the course of this research; to W.J. Burke of AFGL for valuable improvements and comments; to E.G. Holeman of Emmanuel College Physics Research for his essential contribution to the data reduction, and to Professor M.P. Hagan for her continuous support throughout the research.

REFERENCES

Berger, M.J. and S.M. Seltzer, Bremsstrahlung in the atmosphere, J. Atmos. Terr. Phys., 34, 85, 1972.

Imhof, W.L., J.R. Kilner, G.H. Nakano, and J.B. Reagan, Satellite X-ray mappings of sporadic auroral zone electron precipitation events in the local dusk sector, J. Geophys. Res., 85, 3347, 1980.

Imhof, W.L., G.H. Nakano, R.G. Johnson, and J.B. Reagan, Satellite observations of bremsstrahlung from widespread energetic electron precipitation events, J. Geophys. Res., 79, 565, 1974.

Pantazis, J., A. Huber, and M.P. Hagan, Design of a low energy proton spectrometer, AFCRL-TR-75-0637, Final Report, Contract No. F19628-71-C-0060, December 1975.

Walt, M., L.L. Newkirk, and W.E. Francis, Bremsstrahlung produced by precipitating electrons, J. Geophys. Res., 84, 967, 1979.

Whalen, J.A., Auroral oval plotter and nomograph for determining corrected geomagnetic local time, latitude, and longitude for high latitudes in the northern hemisphere, AFCRL-70-0422, Environmental Research Papers, No. 327, July 1970.

LIST OF FIGURES

Figure 1. Typical data record of northern hemisphere showing the anomalous single peak in the polar region. The peak is seen once per 18 second spin from a direction below the satellite's local horizon. The night peak at a particular pitch angle decreases as the pole is approached, and the day peak at a different pitch angle increases as the satellite recedes from the pole.

Figure 2. Polar peak virtually disappears during this time of low magnetic activity (Kp = 2-).

Figure 3. Planetary magnetic three-hour-range indices, December 10, 1975 to April 29, 1976.

Figure 4. Projection of north polar pass of satellite orbits on an invariant latitude, magnetic local time diagram.

Figure 5. Comparison of polar peak observations from dusk side (col. A) with midnight-noon passes (col. B) for high to low Kp index.

Figure 6. A monoenergetic beam of spiraling charged particle radiation having particle velocity v would be observed at $\pm\theta$ pitch angle with respect to magnetic field line B by a detector spinning in a plane.

Figure 7. Theoretical percent of X-rays absorbed in 300 μ silicon (LEPS front detector) due to photoelectric and Compton effects.

Figure 8. The anomalous polar peak reaches an intensity of 2×10^4 counts/sec on this north polar pass, March 26, 1976. Kp = 8-; UT = 9^h.

Figure 9. Surface of earth in the orbit plane under S3-2 north polar orbit track. Pictured are four orbital vantage points of the single peak observation of the obliquely viewed night and day auroral zone. Look angles with respect to the local nadir are labeled.

Figure 10. Variation of polar peak corresponding to four orbital vantage points of Figure 9 (a,b,c,d) and selected from data of Figure 8. Peak always appears in the direction of the night or day aurora.

Figure 11. DMSP satellite image of the visible nighttime continuous aurora plus discrete arcs and bands observed on March 26, 1976. A reference geographic coordinate grid at 100 km altitude overlays the image. The satellite subtrack is shown by a dashed vertical line. The crossing of the equatorward edge of the aurora occurred at 925 UT. The sunset terminator lies at the left of the image.

Figure 12. S3-2 and DMSP satellite tracks plotted on invariant latitude, local geomagnetic time auroral oval nomograph for March 26, 1976, UT 9^h. The image of the aurora from Figure 11 has been sketched in.

Figure 13. The LEPS, at 2886 km away, with an aperture of 46° views an auroral area 15° x $\cdot$ = 1665 km x 2255 km.

Table 1. Energies (MeV) of LEPS Channels

Channel	1	2	3	4	5	6	7	8	9	10	11
Low energy cut off	.082	.123	.165	.232	.345	.477	.680	.948	1.445	2.038	2.927
High energy cut off	.123	.165	.232	.345	.477	.680	.948	1.445	2.038	2.927	6.0

01 ~ 2140

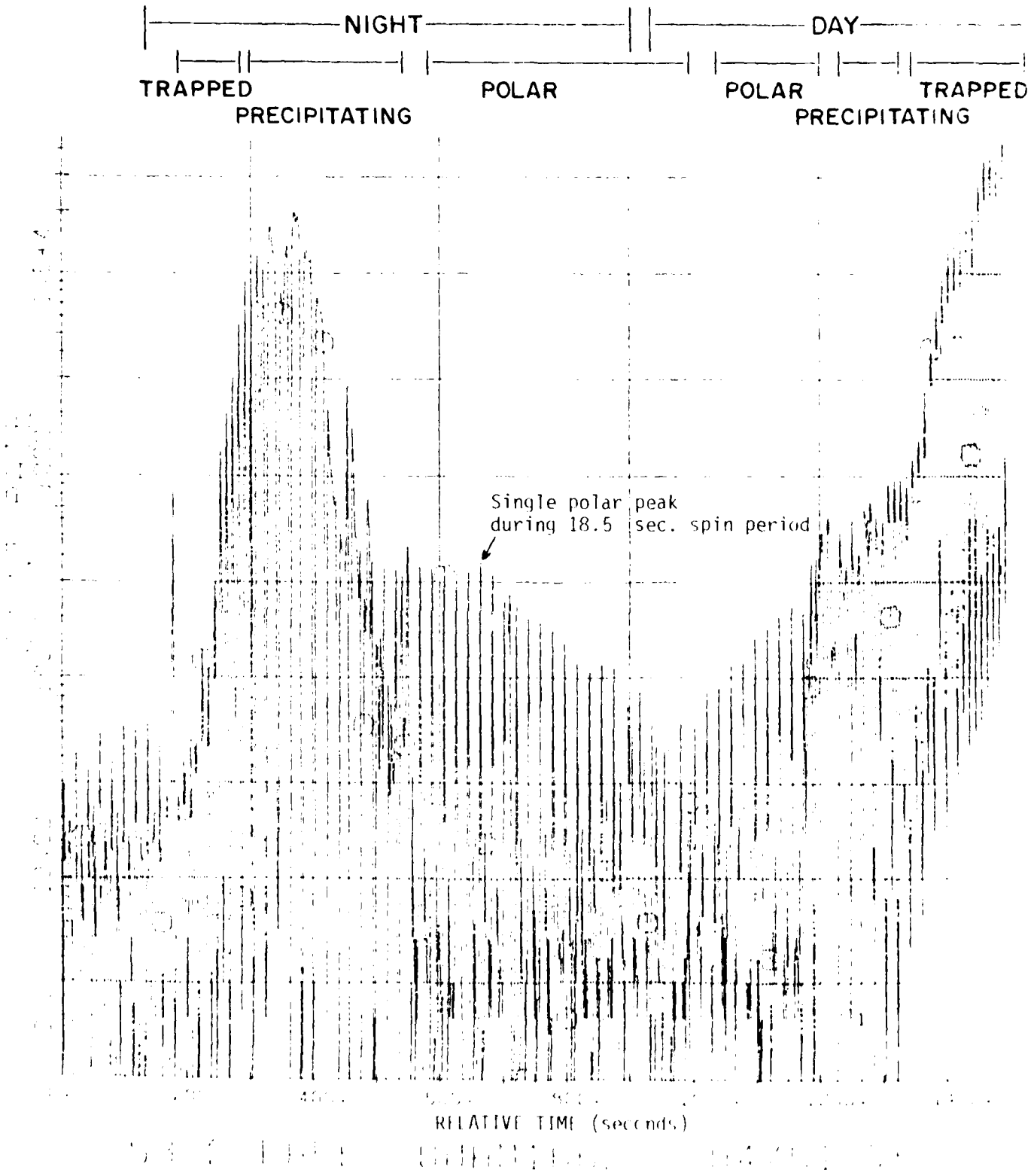

LOW ENERGY CHANNEL 100 KeV

Figure 1.

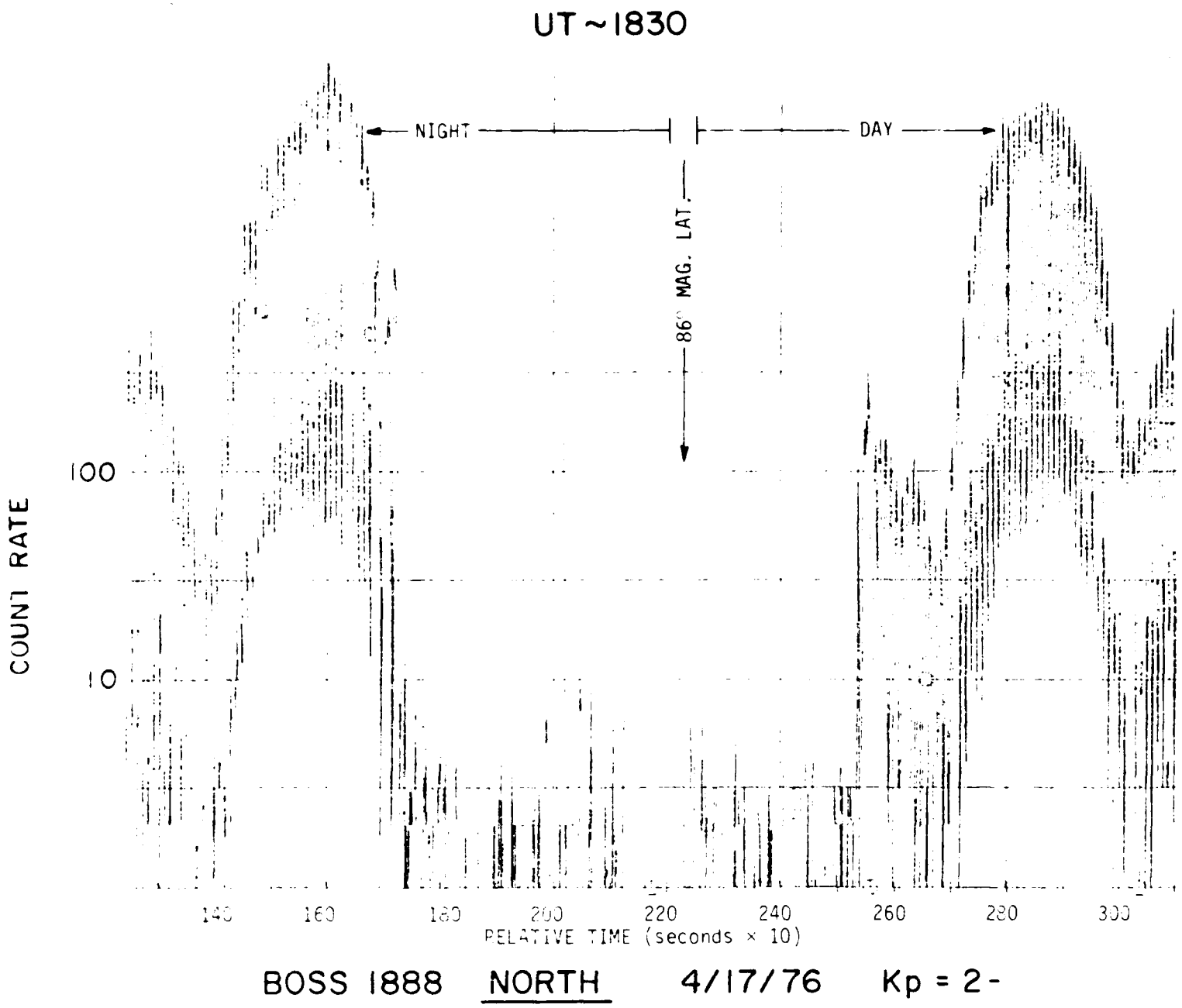
UT ~1830
NIGHT
DAY
86° MAG. LAT.
COUNT RATE
100
10
140
160
180
200
220
240
260
280
300
RELATIVE TIME (seconds × 10)
BOSS 1888 NORTH 4/17/76 Kp = 2-

Figure 2.

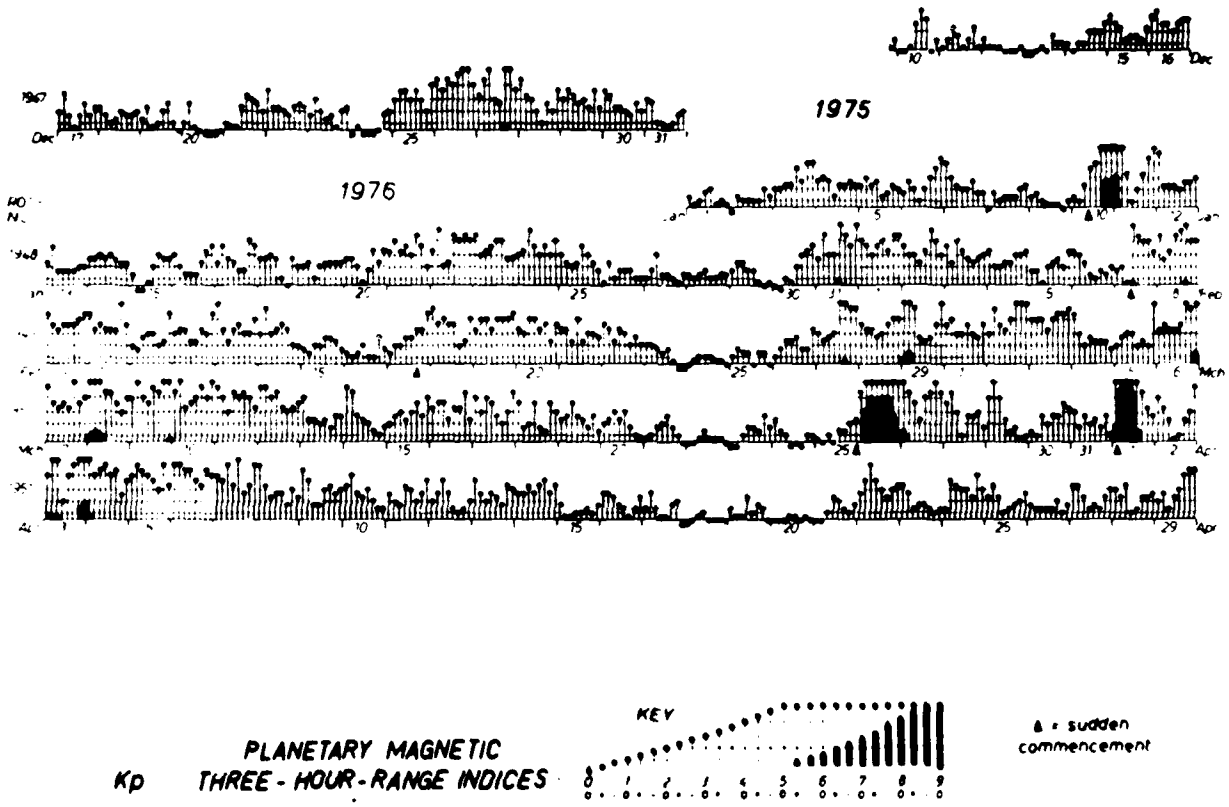
1975
1976
PLANETARY MAGNETIC
Kp THREE - HOUR - RANGE INDICES
KEY
▲ = sudden commencement

Figure 3.

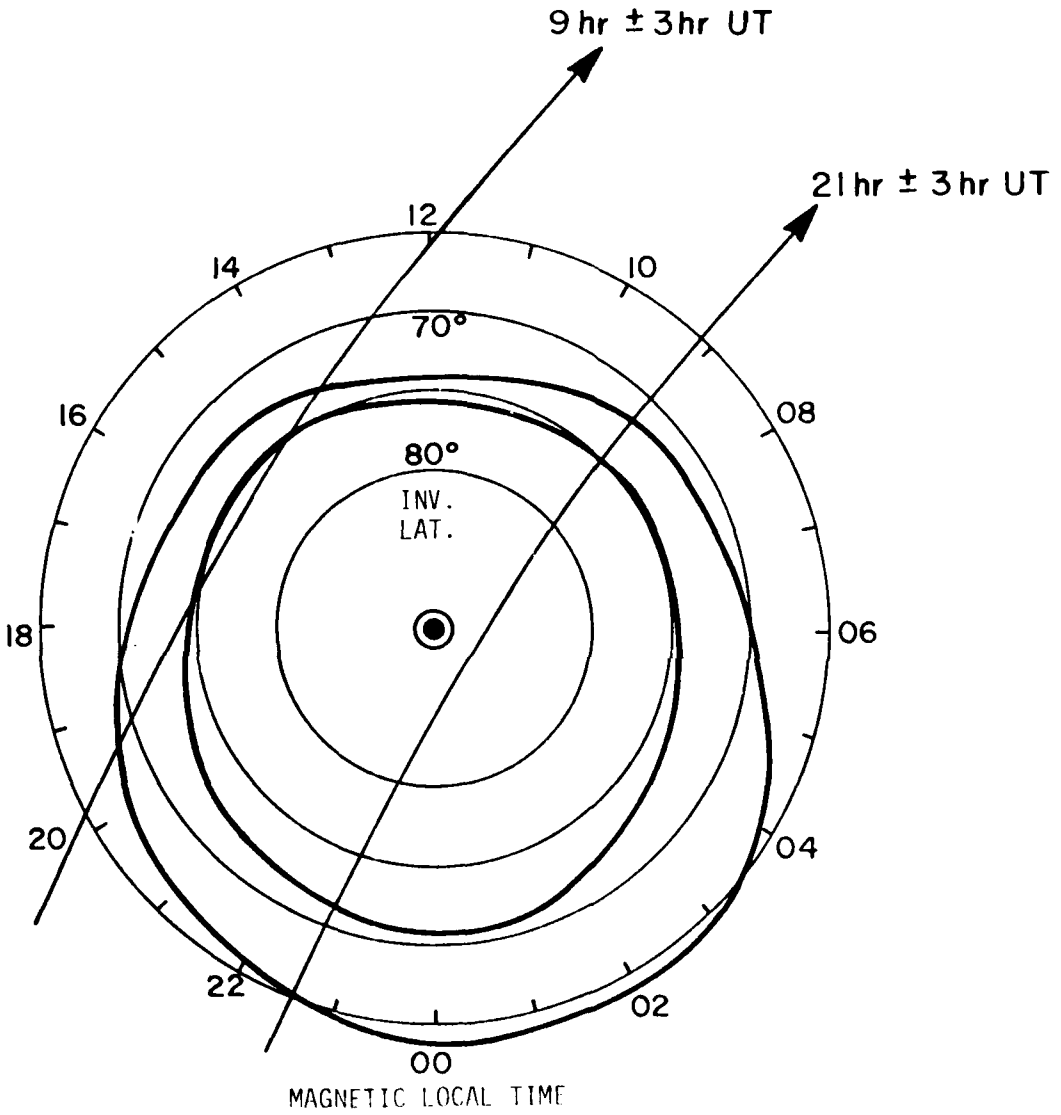
9 hr ± 3 hr UT
21 hr ± 3 hr UT
12
14
10
70°
16
08
80°
INV.
LAT.
18
06
20
04
22
02
00
MAGNETIC LOCAL TIME

Figure 4.

UT ~ 0800 Kp = 8+

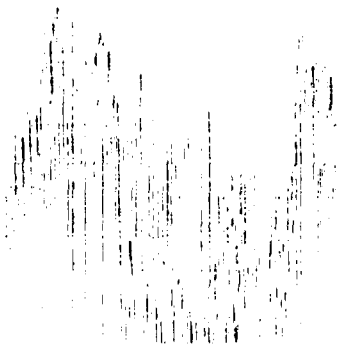

UT ~ 2400 Kp = 4+

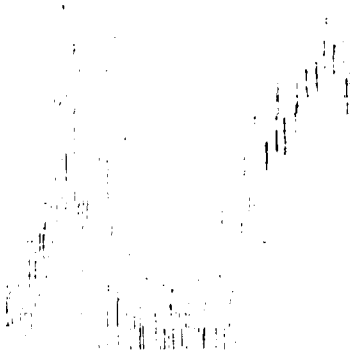

UT ~ 1600 Kp = 5+

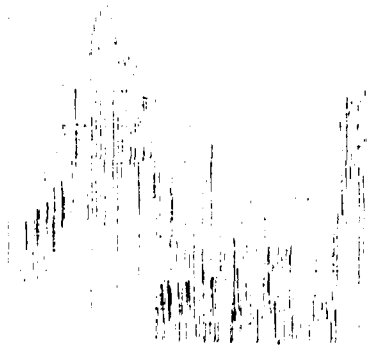

UT ~ 1900 Kp = 4+

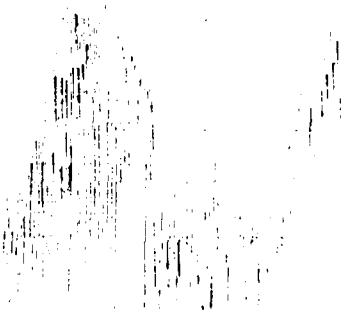

UT ~ 1320 Kp = 3−

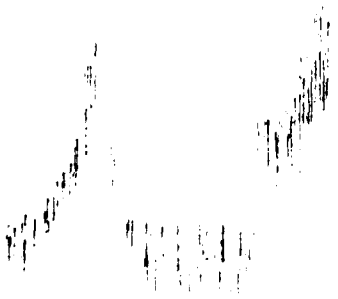

Column A

UT ~ 1830 Kp = 2−

Column B

Figure 5.

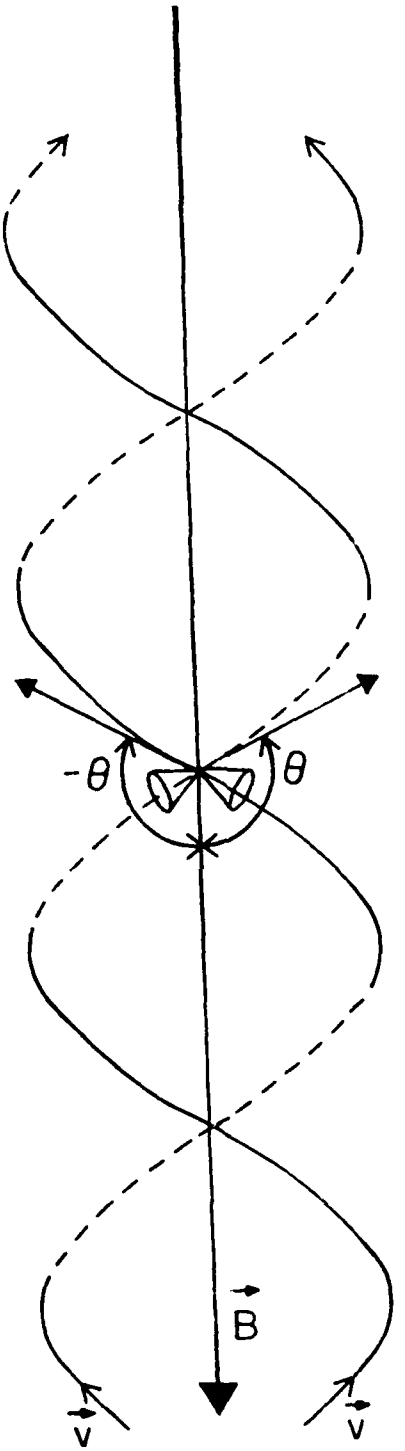

Figure 6.

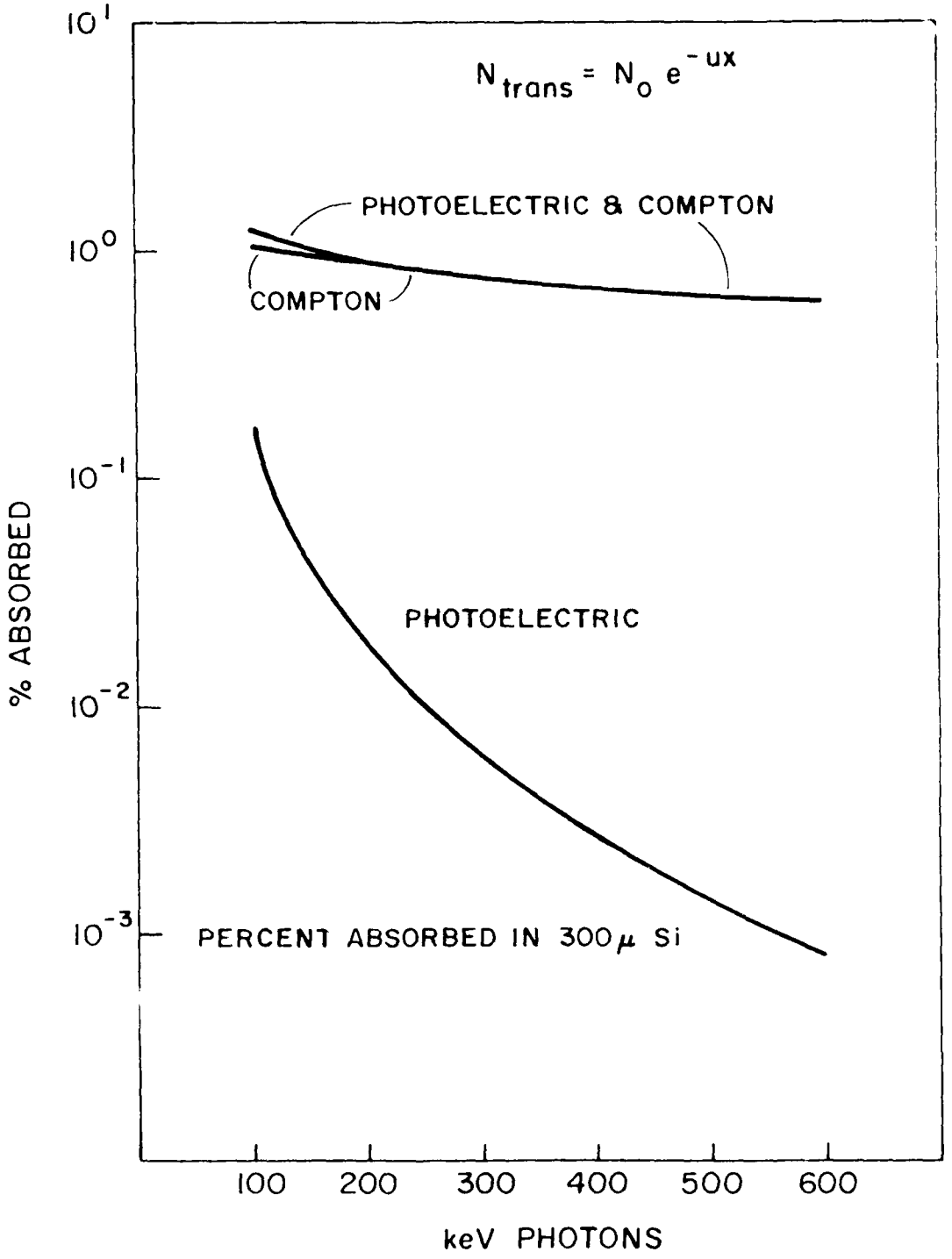
10^1
$N_{trans} = N_o e^{-ux}$
PHOTOELECTRIC & COMPTON
10^0
COMPTON
10^{-1}
% ABSORBED
PHOTOELECTRIC
10^{-2}
10^{-3}
PERCENT ABSORBED IN 300μ Si
100
200
300
400
500
600
keV PHOTONS

Figure 7.

UT = 0900 Kp = 8-

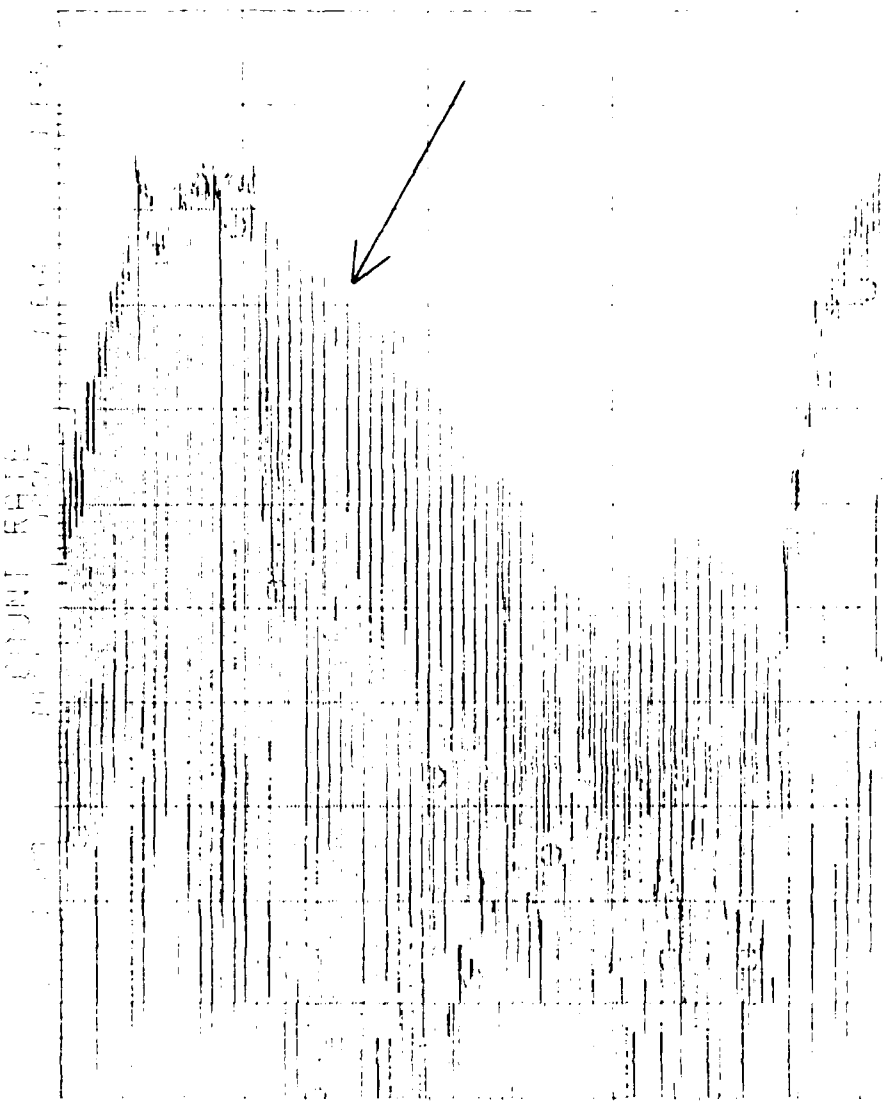

RELATIVE TIME (seconds)

LOW ENERGY CHANNEL 100 keV

Figure 8.

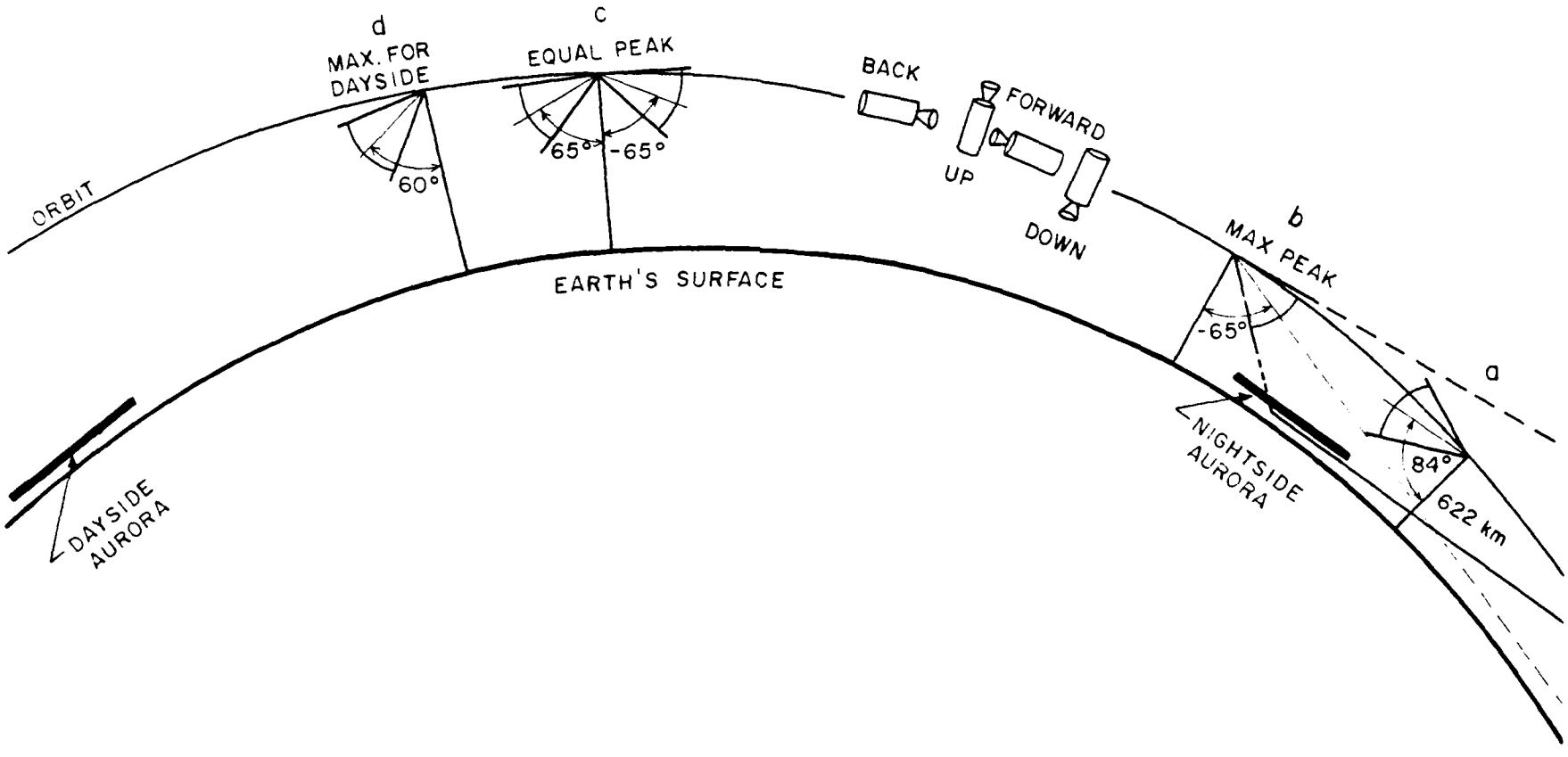
d
MAX. FOR
DAYSIDE
c
EQUAL PEAK
BACK
FORWARD
UP
DOWN
b
MAX PEAK
a
ORBIT
60°
65°
-65°
EARTH'S SURFACE
-65°
84°
622 km
DAYSIDE
AURORA
NIGHTSIDE
AURORA

Figure 9.

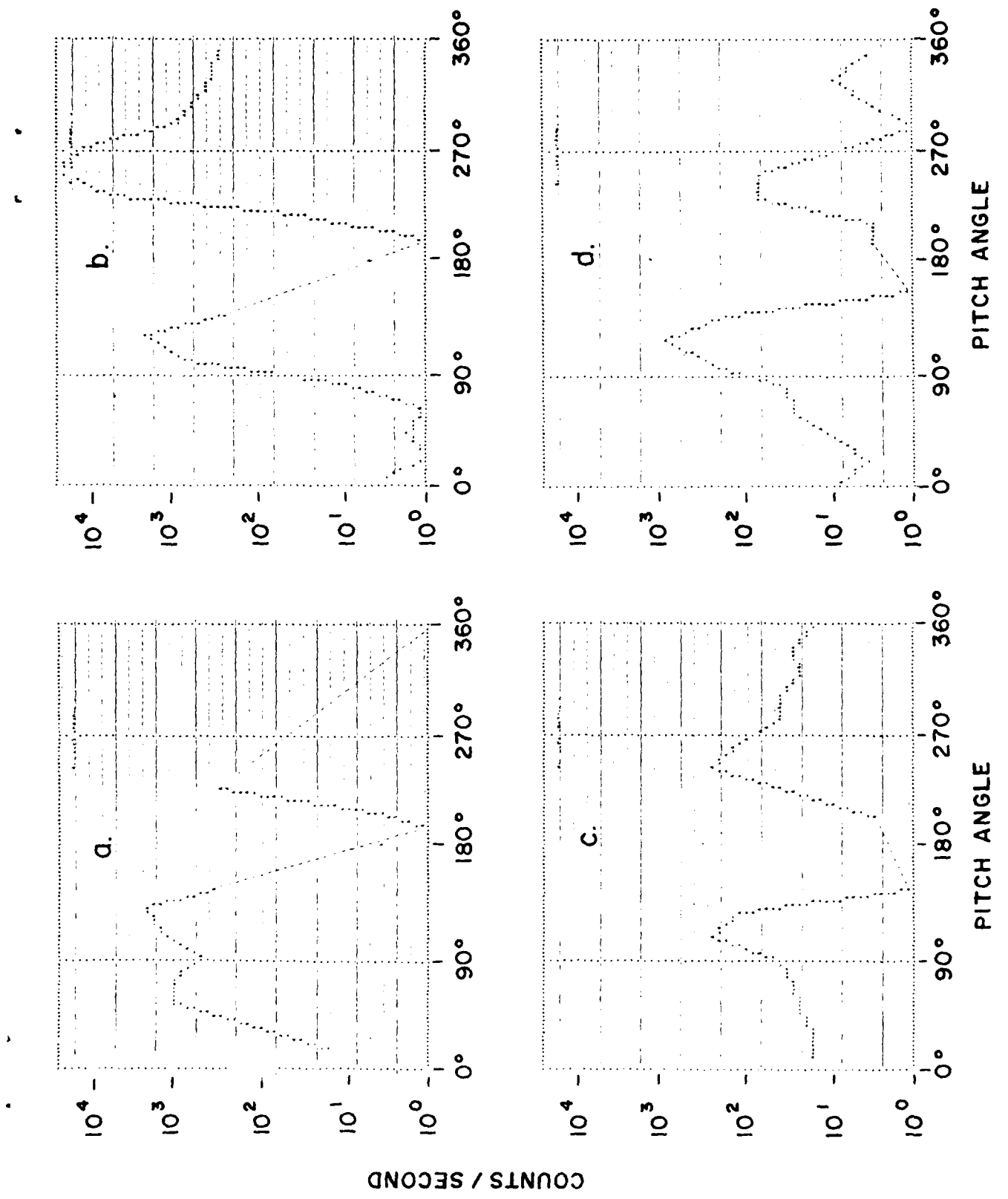
a.
b.
c.
d.
COUNTS / SECOND
PITCH ANGLE
PITCH ANGLE
0°
90°
180°
270°
360°
10^0
10^1
10^2
10^3
10^4

Figure 10.

Figure 11.

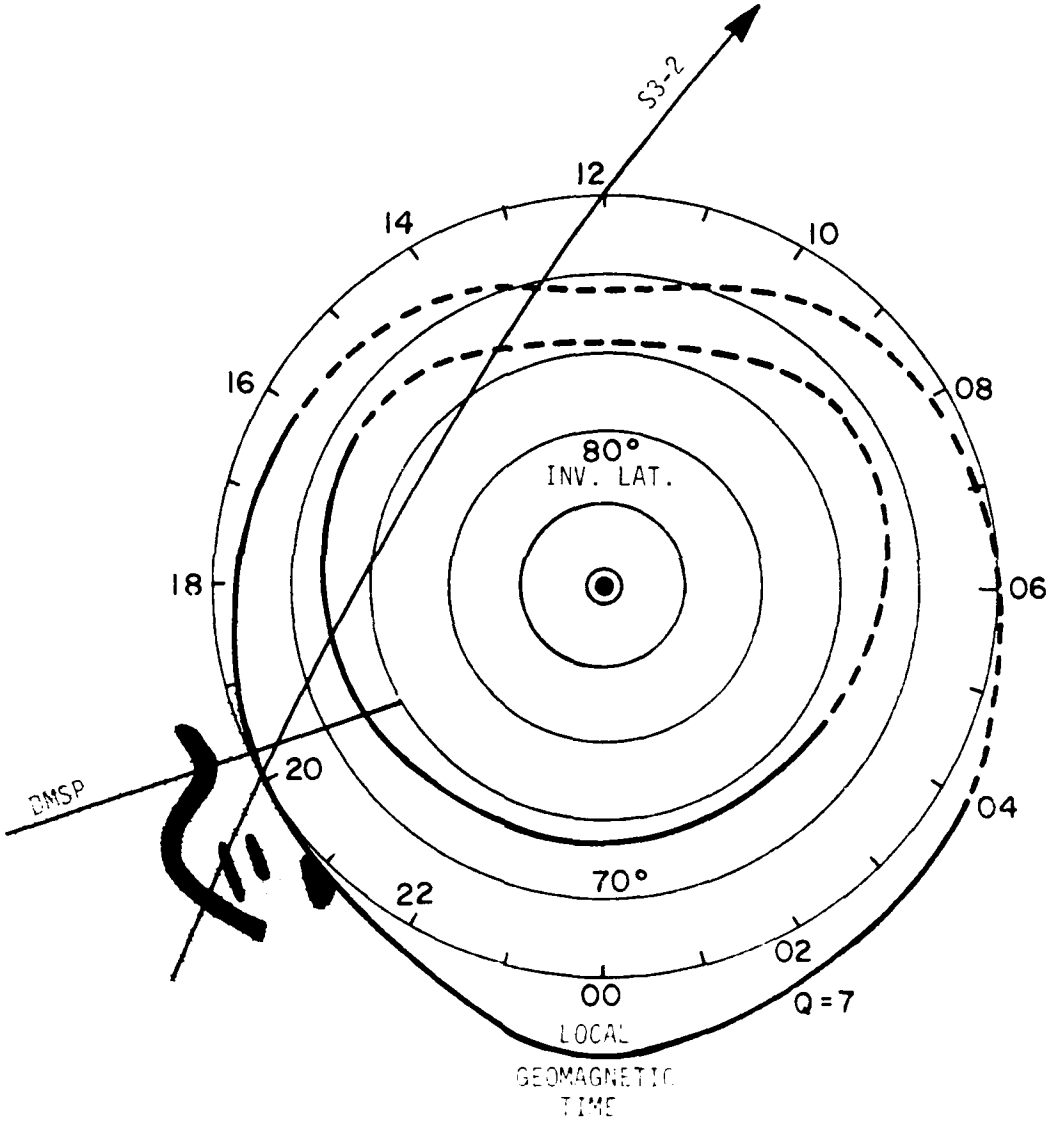
S3-2
12
14
10
16
08
80°
INV. LAT.
18
06
DMSP
20
04
70°
22
02
00
Q=7
LOCAL
GEOMAGNETIC
TIME

Figure 1.

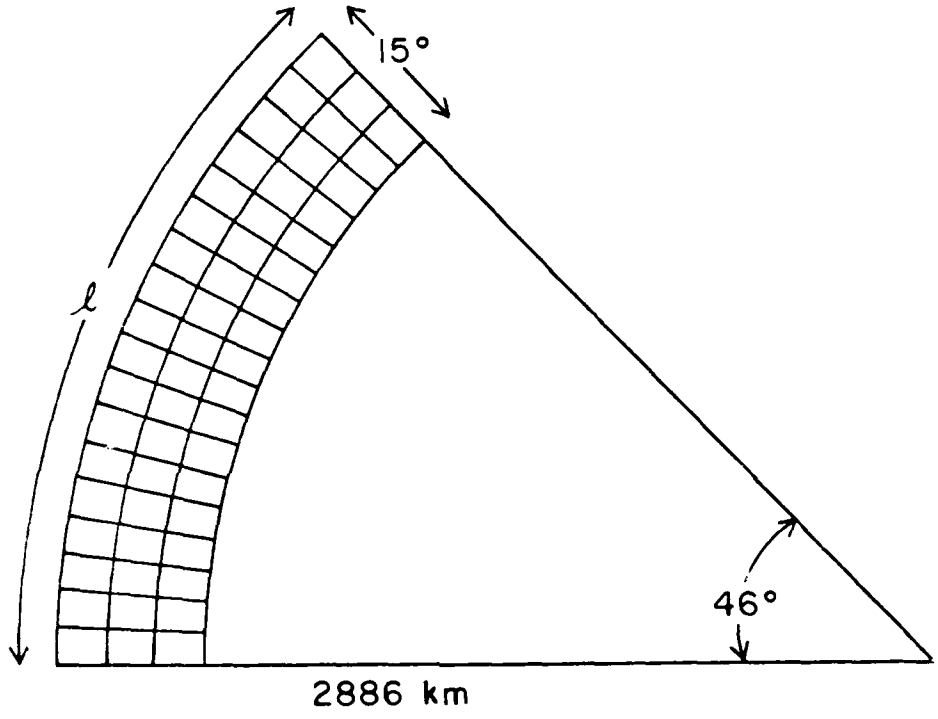

Figure 13.

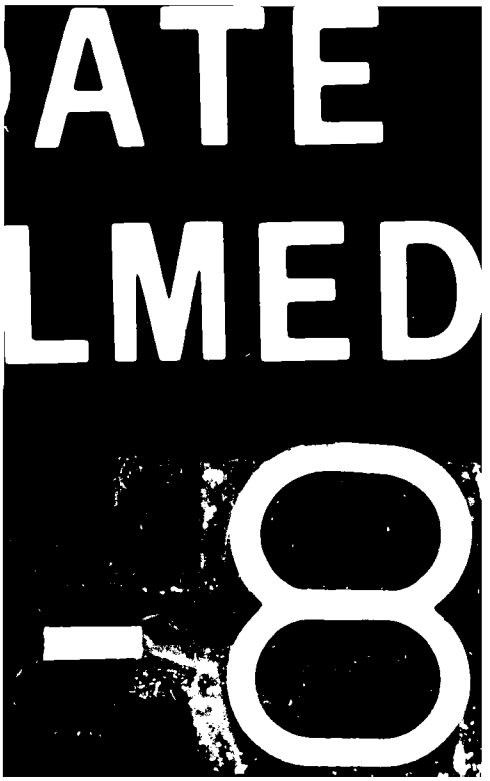
ATE
LMED
-8